

RSC Advances



This is an *Accepted Manuscript*, which has been through the Royal Society of Chemistry peer review process and has been accepted for publication.

Accepted Manuscripts are published online shortly after acceptance, before technical editing, formatting and proof reading. Using this free service, authors can make their results available to the community, in citable form, before we publish the edited article. This *Accepted Manuscript* will be replaced by the edited, formatted and paginated article as soon as this is available.

You can find more information about *Accepted Manuscripts* in the [Information for Authors](#).

Please note that technical editing may introduce minor changes to the text and/or graphics, which may alter content. The journal's standard [Terms & Conditions](#) and the [Ethical guidelines](#) still apply. In no event shall the Royal Society of Chemistry be held responsible for any errors or omissions in this *Accepted Manuscript* or any consequences arising from the use of any information it contains.

Cite this: DOI: 10.1039/c0xx00000x

www.rsc.org/xxxxxx

ARTICLE TYPE

One-pot synthesis of hierarchical WO₃ hollow nanospheres and their gas sensing properties

Chong Wang^a, Changhao Feng^a, Meng Wang^a, Xin Li^a, Pengfei Cheng^b, Hong Zhang^a, Yanfeng Sun^{a*}, Peng Sun^a, Geyu Lu^{a*}

Received (in XXX, XXX) Xth XXXXXXXXX 20XX, Accepted Xth XXXXXXXXX 20XX
DOI: 10.1039/b000000

In this paper, one-pot synthesis of WO₃ hollow sphere nanostructure has been realized via a one-pot template-free solvothermal method. X-ray diffraction patterns demonstrated that the products are pure monoclinic WO₃. Based on the observation of scanning electronic microscopy (SEM) and transmission electron microscopy (TEM), it revealed that the as-prepared WO₃ nanospheres have a diameter of around 2 μ m and are hollow structures with shell thickness about 300 nm which are constructed by numerous oriented nanocrystals. Sensors based on the synthesized WO₃ hollow nanospheres exhibited high to NO₂ at low operating temperature. The detection limit can be as low as ~40 ppb level.

Keywords: solvothermal; tungsten oxide; hollow nanosphere; NO₂ sensor.

1. Introduction

Hollow nanostructures, in addition to its potential application in many fields [1-4], would be very favorable to improve the gas-sensing properties because the rapid and effective diffusion of analyte gases onto the entire sensing surface [5-7]. Thus, it is of great interests to synthesize WO₃ nanocrystals with hollow nanostructure. Up to now, various methods are employed to obtain WO₃ crystal with hollow nanostructure. Li *et al* prepared WO₃ hollow spheres through the hydrolysis of tungsten hexachloride using novel carbon spheres as templates [8]. Chen *et al* reported an acid-treated precursor method to synthesize WO₃ hollow nanostructures [9]. Yoon Ho Cho *et al* prepared WO₃ hollow spheres using the ultrasonic spray pyrolysis method [10]. Among these methods, the complex operation is a negative factor to achieve the final hollow nanostructure. Therefore, a simple, effective and economical method is strongly desired to synthesize WO₃ hollow nanospheres.

As the air pollution is becoming serious, people paid more attention in gas sensors and did excellent work [11-12]. NO₂, as one kind of toxic gases, can affect human health even at parts per million (ppm) levels, such as respiratory system and nerve system [13]. In addition, it could also cause photochemical smog and acid [14]. The Occupational Safety and Health Administration (OSHA) have set a permissible exposure levels for NO_x by 5 ppm [15], and the threshold concentration of NO₂ in air is 3 ppm as listed in the safety standards by the American Conference of Governmental Industrial Hygienists [16]. Thus, there is a strong demand for developing cheap, reliable and sensitive gas sensors targeting NO₂ [17]. Therefore, the excellent response to NO_x makes WO₃ particularly outstanding for monitoring environment pollution and detecting leakage in industrial [18-19]. As a result, much attention has been paid to the synthesis of various

nanostructured WO₃, such as nanowire [20], nanoplate [21], hollow nanosphere [22]. From the viewpoint of sensing, hollow nanospheres attract more interest as they can serve as effective transport channels and active sensing sites for analyte gas molecules, which are crucial for high response and fast response/recovery process [23-24].

In this paper, we report a one-step template-free solvothermal route for the preparation of hierarchical hollow WO₃ nanosphere. This kind of facile chemical route meets the requirements mentioned above and thus obtained WO₃ has promising application in gas sensor area. Characterizations and sensing properties were also reported here. The hollow nanostructures-based gas sensor showed high sensing performances toward NO₂ gas. The results are promising for further application of such hierarchical nanostructures as gas sensor.

2. Experimental

2.1. Synthesis and characterization of hollow nanosphered WO₃

All the reagents (analytical-grade purity) were used without any further purification. In a typical synthesis, 1 g sodium tungstate and 1.2 g citric acid were dissolved in the mixture of distilled water (25 ml) and glycerol (10 ml). After stirring for 20 min, 4 ml 3M HCl was added in the solution drop by drop. Five minutes later, the above solution was transferred into a Teflon-lined stainless steel autoclave, sealed tightly, and maintained at 180°C for 24 h. After the autoclave was cooled to room temperature naturally, the precipitates were washed with deionized water and absolute ethanol for several times using centrifuge, and then dried at 80°C for 24 h. The precipitates were calcined at 500°C for 3 h with a heating rate of 5°C/min. The calcined products were then collected for further analysis.

X-ray power diffraction (XRD) analysis was conducted on a Rigaku D/max-2500 X-ray diffractometer with Cu K α 1 radiation (λ = 1.54056 Å) in the range of 20-60°. The morphology was examined by field-emission scanning electron microscopy (FESEM, JEOL JSM-7500F, operated at an acceleration voltage of 15 kV). Transmission electron microscopy (TEM), selected-area electron diffraction (SAED) were obtained on a JEOL JEM-2100 microscope operated at 200 kV.

2.2. Fabrication and measurement of sensor

The calcined powders were mixed with ethanol to form a paste which was then coated onto an alumina tube (4 mm in length, 1.2 mm in external diameter and 0.8 mm in internal diameter) using a small brush slowly and lightly. The tube was installed with a pair of gold electrodes, and each electrode was connected with two Pt wires. After brushing, a thick film was formed. After drying at room temperature, the sensing device was

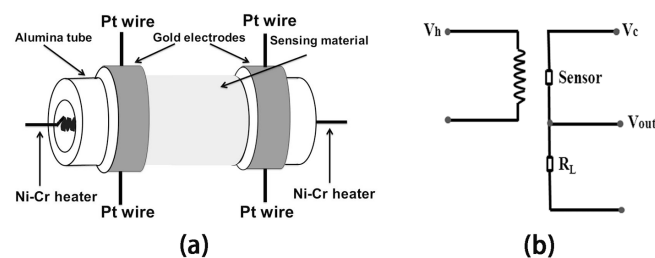


Fig. 1. (a) Schematic structure of the gas sensor. (b) Diagram of sensor and measurement electric circuit

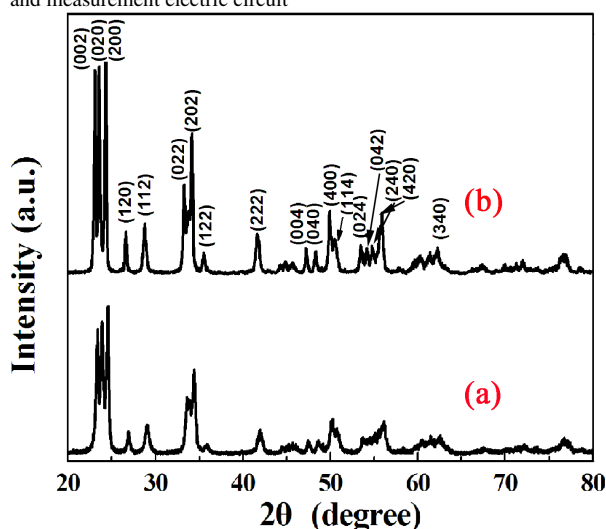


Fig. 2. X-ray diffraction patterns of the sintered product before (a) and after sintering (b).

then sintered at 300 °C for 2 h in air. Finally, a Ni–Cr alloy coil was inserted into the alumina tube as a heater in order to control the operating temperature of the sensor. A schematic structure of the as-fabricated sensor was shown in Fig. 1a.

The electrical resistance of the sensor was measured in air and in target gas, respectively. The response of the sensor is defined as $S=R_g/R_a$ for oxidizing gas or R_a/R_g for reducing gas, here, R_a and R_g are the resistances of the sensor in the air and target gas, respectively. The response time and recovery time are defined as the time taken by the sensor to achieve 90% of the total resistance change during the adsorption and desorption process, respectively. The schematic of electric circuit was shown in Fig. 1b.

3. Results and discussion

3.1. Structural and morphological characteristics of the as-obtained WO₃

The typical XRD patterns of the products before and after sintering are shown in Fig. 2a and Fig. 2b. Both of the diffraction peaks can be well indexed to pure monoclinic WO₃ (JCPDS file no. 72-1465). No peaks of other impurity phases are detected from the patterns, indicating the high purity of the product.

From a magnified SEM image (Fig. 3a), it can be seen that the sample possesses a hollow nanosphere structure with an average diameters of about 2 μm. Some microspheres with broken holes can also be observed and provide the direct evidence that the as-prepared WO₃ nanospheres are hollow structure in nature. Enlarged SEM image of single cracked hollow nanosphere is presented in Figure 3b, further confirming its hollow structure. Furthermore, it displays that the shell of the hierarchically hollow spheres consists of organized WO₃ nanocrystals.

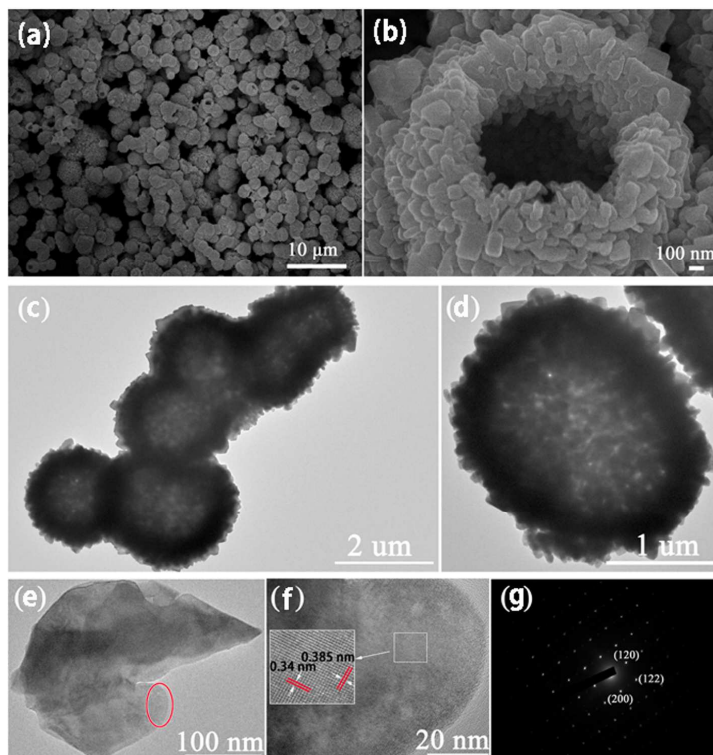


Fig. 3. (a) and (b) Typical SEM images of WO₃ product, (c) TEM images of the hierarchical WO₃ hollow nanospheres, (d) a typical nanosphere, (e) an individual nanosheet from the cracked nanosphere, (f) HRTEM image of a part of the nanosheet in (e), (g) the corresponding SAED patterns of the WO₃ nanosheet.

In addition, the WO₃ product was further characterized by TEM, and the corresponding TEM images are shown in Figure 3c and 3d. The obvious contrast between the dark edge and the relatively bright center confirms its hollow nature. From the detailed observation in Figure 3d, it can be observed that the shell thickness is about 300 nm. The TEM image of an individual nanocrystal is shown in Figure 3e. The HRTEM image of the part of the individual nanocrystal is presented in Fig. 3f. The clearly resolved lattice fringes in the HRTEM images confirmed the high crystallinity of the nanocrystal. The space between adjacent lattice planes along a certain direction is 0.34 nm, whereas the space between adjacent lattice planes along the other direction is 0.385 nm. They are found to correspond to (120) and (002) planes of monoclinic WO₃ crystal (JCPDS No. 72-1465), respectively. The selected area electron diffraction (SAED) patterns result is shown in Fig. 3g, which indicates that the nanocrystals of monoclinic WO₃ are single crystalline.

The nitrogen adsorption and desorption measurements were performed to evaluate the porosity and surface area of the as-synthesized WO₃ structures. The nitrogen adsorption and desorption isotherm plots and corresponding pore-size distribution plots of the hierarchical WO₃ hollow structures are given in Fig. 4. From the curves, we can see that this sample has two obvious peaks at the pore-size distribution plot about 2.7 nm and 48.7 nm respectively, displays porous structures with a wide range of pore size distributions from 1.7 nm to 167 nm, which is beneficial for the target gas to adsorb on the sensing layer. The BET surface area of the product was calculated to be 5.4584 m²/g.

To reveal the growth process of hollow nanosphered WO₃ and possible growth mechanism, a series of experiments depending on different reaction times were performed. When the reaction time was only 10 min, no precipitate could be obtained. As increased the reaction time to 15 min, some precipitates

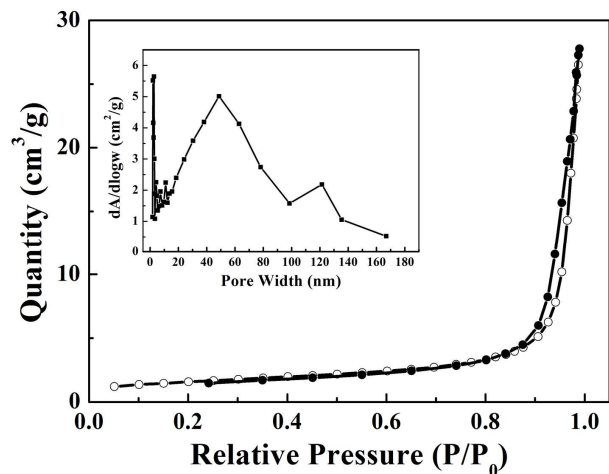


Fig. 4. Nitrogen adsorption-desorption isotherm and corresponding pore-size distribution of as-synthesized WO_3 sample.

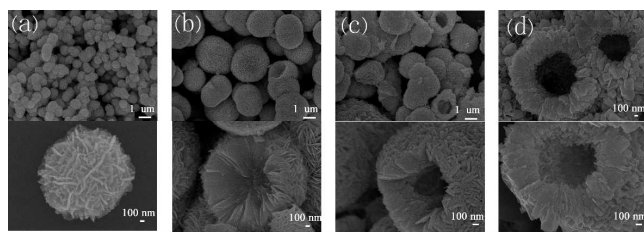


Fig. 5. FESEM images of the morphology evolution at different reaction times: (a) 15 min, (b) 45 min, (c) 1 h and (d) 24 h.

emerged and the morphology results are shown in Fig. 5a. The 3D solid nanospheres with oriented nanosheets can be observed. The diameter of the sphere was about 1 μm . Following the Gibbs law, the dissolving nanoparticles further aggregated onto the solid nanospheres through an oriented attachment in order to minimize the total surface energy, as shown in Fig. 5b. The diameter of the nanosphere became bigger obviously ($\sim 2 \mu\text{m}$). When the reaction time was prolonged to 1 h, hollow structures appeared among the solid nanospheres (Fig. 5c). As the reaction time was extended to 24 h, all the solid nanospheres transformed into hierarchical hollow nanostructures finally (Fig. 5d). We consider that the evolution of morphology can be explained by Ostwald ripening mechanism [25,26], in which a classic phenomenon in particle growth involves the growth of larger particles at the cost of smaller particles due to the higher solubility of smaller particles. In the initial stage, solid nanoparticles as precursors are formed. With the consuming of the reactants, full nanospheres formed. With the reaction processed, the inner particles, which possess nanoscaled diameter and higher surface energy, would dissolve and transfer to the outer space, forming the inner hollow nanostructures at last.

3.2. Gas-Sensing Properties for NO_2

Sensing properties of the sensor based on the hollow nanosphered WO_3 samples were investigated. It is well known that the response of a gas sensor is highly influenced by the operating temperature [27]. The correlation of the gas response of the sensor to 1 ppm NO_2 and the operating temperature was tested, and the result is shown in Fig. 6. As a comparison, sensor based on commercial WO_3 was also measured. It is obvious that the hierarchical hollow nanostructures exhibited superior response over the commercial WO_3 . As can be seen that the response increases with a raise of operating temperature and reaches the maximum value at 100°C . When the temperature is

further increased, the response decreases gradually, indicating that the response is greatly influenced by temperature.

This phenomenon can be explained as follows: the increase of the response can be attributed to the increase of the surface reaction ($\text{NO}_{2(g)} + e^- \rightarrow \text{NO}_{2(\text{ads})}^-$). Such adsorption can capture the electrons from WO_3 and resulting in the increasing of the electrical resistance. However, when the temperature is higher, larger amount of oxygen molecules dissociate and adsorb on the active sites, resulting in the decrease of the free active sites for the adsorption of NO_2 . On the other hand, the rate of adsorption is lower than desorption at such higher temperature [25,28,29]. Therefore, 100°C was chosen for the optimum working temperature of the sensor. The four reversible cycles of the response curve indicates a stable and repeatable characteristic, as shown in the inset of Fig. 7, the response time and recovery time were about 237 s and 88 s, respectively. Fig. 8a displays the response-recovery curves of the sensors to NO_2 with concentrations varying from 40 to 4000 ppb at optimum operating temperature. The resistance of the sensor increases upon exposure to NO_2 , whereas it decreases upon the removal of NO_2 . The response of the sensor increased with the increase of gas concentrations. The profile of the sensor response as a function of NO_2 gas concentrations is shown in Fig. 8b. It is interesting to note that the response of the sensor to 40 ppb NO_2 is about 3.4, which demonstrates that the sensor exhibits an acceptable response from the view of practical application. A comparison of the sensing performances between the sensor fabricated in this work and literature reports is summarized in Table 1. From the table, it can be observed that the sensor based on WO_3 hollow nanospheres has a correspondingly high gas response and low working temperature. These results demonstrate that the hollow nanosphered WO_3 -based sensor has a quite high response to NO_2 and a relative low working temperature.

The long-term stability of the gas sensor is a relative crucial parameter in the view of practical application. The response as a function of the number of testing days was also measured and shown in Fig. 9. The response of the sensor to 1 ppm NO_2 at 100°C was nearly constant during two weeks, which indicated the splendid long-term stability of the sensor based on WO_3 hollow nanospheres.

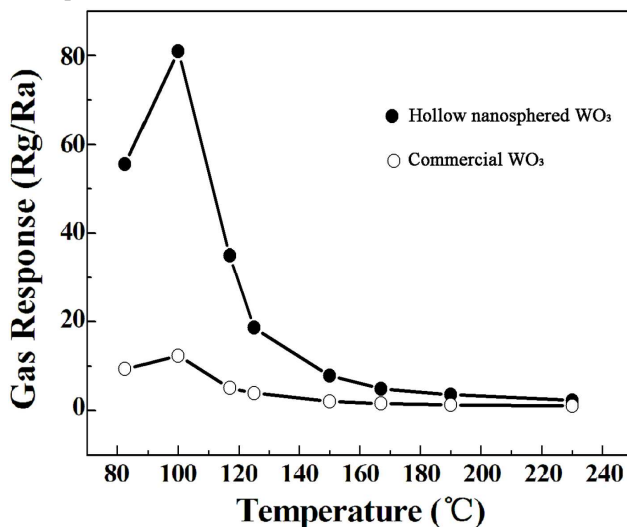


Fig. 6. Correlations between the gas response to 1 ppm NO_2 and the operating temperature for hollow nanosphered WO_3 and commercial WO_3 .

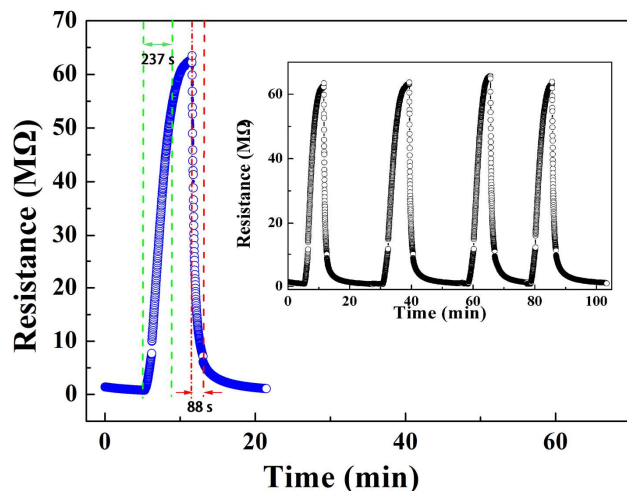


Fig. 7. Four periods of response curve to 1 ppm NO₂ at 100°C.

WO₃ is a typical n-type semiconductor, and its gas-sensing mechanism belongs to the surface-controlled type. In air ambient, oxygen molecules are adsorbed onto the surface of the as-synthesized WO₃ and generate the chemisorbed oxygen species (O₂⁻, O⁻ and O²⁻) by capturing electrons from the conduction band of WO₃, depletion region is formed on the surface area of WO₃ [27]. Upon exposure to NO₂ gas, the NO₂ gas molecules are directly adsorbed on the active sites on tungsten oxide surface. Charge transfer is likely to occur from WO₃ to adsorbed NO₂ because of the strong electron-withdrawing power of the NO₂ molecules, resulting in the large increase in electrical resistance. The special hierarchical hollow nanosphere structure, which is beneficial for the rapid and effective diffusion of analyte gases onto the entire sensing material, might be the reasons for the high response of the sensor to NO₂. Therefore, the sensor is expected to have high response to NO₂.

As is well known that the selectivity is another important parameter of a sensor in the view of practical application. Therefore, at the optimum operating temperature, the response of the sensor based on the hierarchical hollow nanosphere to various kinds of gases was investigated, such as Cl₂, CO, H₂S, NH₃, acetone and ethanol, as shown in Fig. 10. It can be seen that the sensor has a high response to NO₂ compared to the other gases. Such result demonstrates that the sensor using the WO₃ nanostructure synthesized here exhibits an excellent selectivity to NO₂ against the other tested gases at the working temperature of 100°C.

4. Conclusion

In summary, hierarchical WO₃ hollow nanosphere has been successfully synthesized through a simple one-step solution route. Field emission scanning electron microscopic and transmission electron microscopy results demonstrate that the products are composed of numerous nanocrystals. In addition, gas sensing properties of sensors based on the hollow WO₃ hollow toward NO₂ were investigated. The sensor exhibits excellent NO₂ sensing properties at 100°C. These results indicate that our sensor might have potential application to fabricate highly sensitive NO₂ gas sensor devices.

This work is supported by Application and Basic Research of Jilin Province (20130102010JC), the National Nature Science Foundation of China (No. 61304242, 61327804, 61134010, 61377058 and 61374218), Program for Chang Jiang Scholars and

Innovative Research Team in University (No. IRT13018) and “863” High Technology Project (2013AA030902).

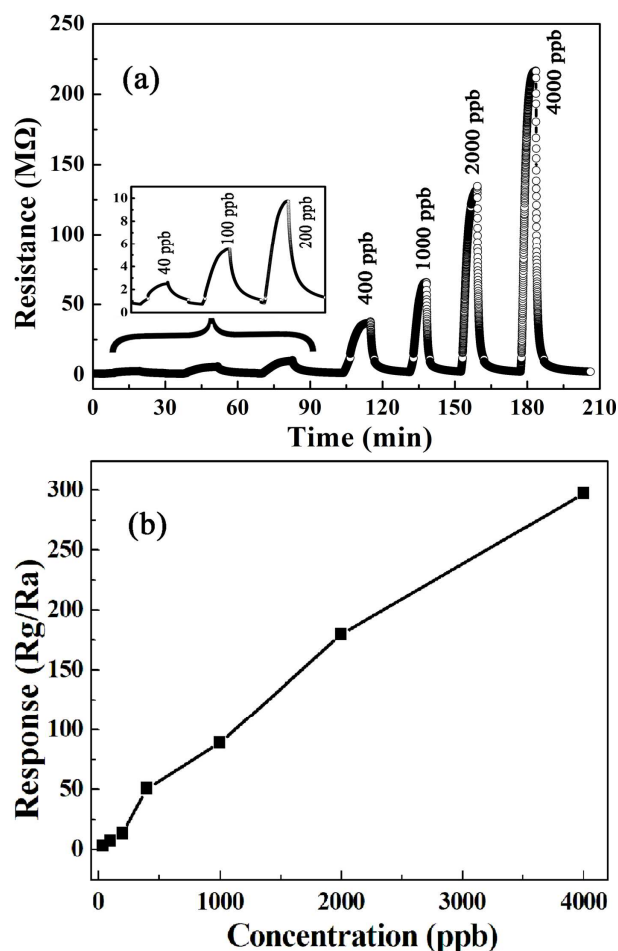


Fig. 8. (a) Response transients of the sensor to different NO₂ concentration at 100°C. (b) Gas response of the sensor as a function of NO₂ concentrations.

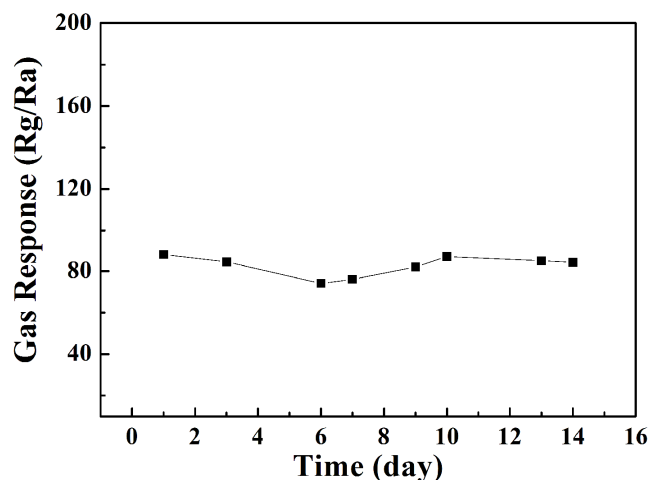
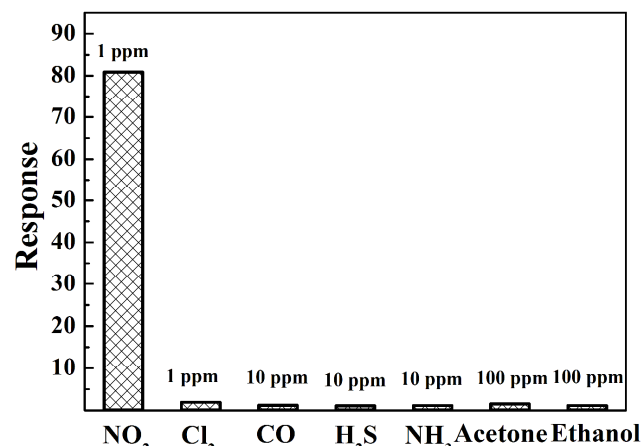


Fig. 9. Stability of the sensor based on as-prepared sample at 100°C.

Table 1 Gas responses to NO₂ in the present study and those reported in the literatures

Material	Preparation	NO ₂ concentration	Operating temperature	Response	Reference
WO ₃	Hydrothermal	1 ppm	100 °C	89	Present study
WO ₃	Hydrothermal	1 ppm	300 °C	54	[22]
WO ₃	Ultrasonic spray pyrolysis	1 ppm	300 °C	4.8	[10]
WO ₃	Hydrothermal	1 ppm	300 °C	5.3	[25]

Fig. 10. Comparison of responses of the sensor based on WO₃ to various gases at 100 °C.

Notes and references

a: State Key Laboratory on Integrated Optoelectronics, College of Electronic Science and Engineering, Jilin University, Changchun 130012, People's Republic of China. Fax: +86 431 85167808; Tel: +86 431 85167808; E-mail: syf@jlu.edu.cn, luyg@jlu.edu.cn

b: School of Aerospace Science and Technology, Xidian University, Xi'an 710126, People's Republic of China.

References

- [1] H. Huang, E.E. Remsen, *J. Am. Chem. Soc.*, 1999, 121, 3805-3806.
- [2] W. Meier, *Chem.Soc. Rev.*, 2000, 29, 295-303.
- [3] P.F. Cheng, P. Sun, S.S. Du, Y.X. Cai, X.W. Li, Zhenyu Wang, F.M. Liu, J. Zheng and G.Y. Lu, *RSC Adv.*, 2014, 4, 23396-23404.
- [4] X.W. Li, W. Feng, Y. Xiao, P. Sun, X.L. Hu, K. Shimanoe, Geyu Lu and N. Yamazoe, *RSC Adv.*, 2014, 4, 28005-28010.
- [5] N. Du, H. Zhang, B.D. Chen, X.Y. Ma, Z.H. Liu, J.B. Wu and D.R. Yang, *Adv. Mater.*, 2007, 19, 1641-1645.
- [6] H.G. Zhang, Q.S. Zhu, Y. Zhang, Y. Wang, L. Zhao and B. Yu, *Adv. Funct. Mater.*, 2007, 17, 2766-2771.
- [7] M. Tiemann, *Chem. Eur. J.*, 2007, 13, 8376-8388.
- [8] X.L. Li, T.J. Lou, X.M. Sun, and Y.D. Li, *Inorg. Chem.*, 2004, 43, 5442-5449.
- [9] D. Chen and J.H. Ye, *Adv. Funct. Mater.*, 2008, 18, 1922-1928.
- [10] Y.H. Cho, Y.C. Kang, J.H. Lee, *Sens. Actuators, B*, 2013, 176, 971-977.
- [11] S. Agarwala, W. L. Ong and G. W. Ho, *Sci. Adv. Mater.*, 2013, 5, 1418-1426
- [12] S. Agarwala, Z. H. Lim, E. Nicholson and G. W. Ho, *Nanoscale*, 2012, 4, 194-205
- [13] B.T. Marquis, J.F. Vetelino, *Sens. Actuators, B*, 2001, 77, 100-110.
- [14] G. Eranna, B.C. Joshi, D.P. Runthala, R.P. Gupta, *Crit. Rev. Solid State Mater. Sci.*, 2004, 29, 111-188.
- [15] OSHA and MSHA Diesel Exposure Limit (2006)
- [16] M. Penza, C. Martucci, G. Cassano, *Sens. Actuators, B*, 1998, 50, 52-59.
- [17] Y. Shimizu, H. Nishi, H. Suzuki, K. Maeda, *Sens. Actuators, B*, 2000, 65, 141-143.
- [18] B. Deb, S. Desai, G.U. Sumanasekera and M.K. Sunkara, *Nanotechnology*, 2007, 18, 285501.
- [19] C. Cantalini, H.T. Sun, M. Faccio, M. Pelino, S. Santucci, L. Lozzi, M. Passacantando, *Sens. Actuators, B*, 1996, 31, 81-87.
- [20] Y.M. Zhao, Y.Q. Zhu, *Sens. Actuators, B*, 2009, 137, 27-31.
- [21] K.F. Wang, P.F. Zeng, J. Zhai, Q.Q. Liu, *Electrochem. Commun.*, 2013, 26, 5-9.
- [22] C.Y. Lee, S.J. Kim, I.S. Hwang, J.H. Lee, *Sens. Actuators, B*, 2009, 142, 236-242.
- [23] J.H. Lee, *Sens. Actuators, B*, 2009, 140, 319-3369.
- [24] D.W. Wang, S.S. Du, X. Zhou, B. Wang, J. Ma, P. Sun, Y.F. Sun and G.Y. Lu, *CrystEngComm*, 2013, 15, 7438.
- [25] X.Q. An, J.C. Yu, Y. Wang, Y.M. Hu, X.L. Yu, G.J. Zhang, *J. Mater. Chem.*, 2012, 22, 8525-8531.
- [26] W. Z. Ostwald, *Phys. Chem.*, 1897, 22, 289
- [27] N. Yamazoe, G. Sakai and K. Shimanoe, *Catal. Surv. Asi*, 2003, 7, 63-75.
- [28] B. Ruhland, T. Becker, G. Müller, *Sens. Actuators, B*, 1998, 50, 85-94.
- [29] A.P. Lee, B.J. Reedy, *Sens. Actuators, B*, 1999, 60, 35-42.

A simple solvothermal method was used to the synthesis of hollow nanosphered WO_3 , which exhibited a good response to NO_2

